Folding−Unfolding Equilibrium and Kinetics of Equine β-Lactoglobulin: Equivalence between the Equilibrium Molten Globule State and a Burst-Phase Folding Intermediate†

Kazuo Fujiwara,‡ Munehito Arai,§ Akio Shimizu,‡ Masamichi Ikeguchi,*,‡ Kunihiro Kuwajima,§ and Shintaro Sugai‡

Department of Bioengineering, Faculty of Engineering, Soka University, 1-236 Tangi-cho, Hachioji, Tokyo 192-8577, Japan, and Department of Physics, School of Science, University of Tokyo, 7-3-1 Hongo, Bunkyou-ku, Tokyo 113-8654, Japan

Received November 10, 1998; Revised Manuscript Received January 25, 1999

ABSTRACT: The denaturant-induced equilibrium unfolding transition of equine β-lactoglobulin was investigated by ultraviolet absorption, fluorescence, and circular dichroism (CD) spectra. An equilibrium intermediate populates at moderate denaturant concentrations, and its CD spectrum is similar to that of the molten globule state previously observed for this protein at acid pH [Ikeguchi, M., Kato, S., Shimizu, A., and Sugai, S. (1997) *Proteins: Struct., Funct., Genet. 27*, 567−575]. The unfolding and refolding kinetics were also investigated by the stopped-flow CD and fluorescence. A significant change in the CD intensity was observed within the dead time of measurements (25 ms) when the refolding reaction was initiated by diluting the urea-unfolded protein solution, indicating the transient accumulation of the folding intermediate. The CD spectrum of this burst-phase intermediate agrees well with that of the molten globule state at acid pH. The stability of the burst-phase intermediate was also estimated from the urea-concentration dependence of the burst-phase amplitude, and it shows a fair agreement with that of the equilibrium intermediate. These results indicate that the molten globule state of equine β-lactoglobulin populates at moderate urea concentration as well as at acid pH and it is equivalent with the kinetic folding intermediate.

β-Lactoglobulin is a member of the lipocalin family, which is a subgroup of the calycin superfamily (*1*−*3*). The proteins that belong to the calycin superfamily share the up-and-down β-barrel structure (*1*−*3*). Although a large number of proteins are known to belong to the lipocalin family, little is known about the folding mechanism of lipocalins.

Previously, we have investigated the folding reaction of bovine β-lactoglobulin (BLG)[1] as a model protein to study the folding mechanism of lipocalins and observed the accumulation of a burst-phase intermediate within the dead time of the stopped-flow CD measurements (*4*, *5*). The intermediate shows a far-UV CD spectrum with a higher intensity than that of the native state, and an analysis of the CD spectrum of the intermediate has indicated the formation of nonnative α-helices in the intermediate, although the nativelike β-sheet structure may also be present in the intermediate. Similar observations have been reported by Hamada et al. (*6*). A recent stopped-flow small-angle X-ray scattering (SAXS) experiment has also revealed that the burst-phase intermediate in the folding of BLG has a compact and globular shape (*7*). Thus, the burst-phase intermediate in the folding of BLG has properties characteristic of the molten globule (MG) state, i.e., substantial secondary structures and a compact shape (*8*, *9*). However, the presence of nonnative α-helices in this intermediate is unique for BLG because this has not been observed in the MG states of other proteins. It is thus important for our understanding of the β-lactoglobulin folding to address the issue of whether the nonnative α-helices formed in the burst-phase intermediate play a crucial role in directing the subsequent folding processes. As the first step in clarifying this issue, it is essential to determine the structure of the burst-phase intermediate of β-lactoglobulin, especially to determine the positions in which nonnative α-helices are formed.

Recently, we have also found that equine β-lactoglobulin (ELG) assumes a stable MG state at pH 1.5, in which nonnative α-helices are formed (*10*). ELG consists of 162 amino acids with two disulfide bridges as well as BLG. However, the amino acid sequence of ELG is surprisingly different from that of BLG; 72 amino acids (44%) are different (*11*). ELG is monomeric at any pH investigated (*10*), whereas BLG shows various oligomeric states depending on pH (*12*). ELG has no free cysteine residue, whereas BLG has a free cysteine residue and disulfide interchange readily occurs (*13*). These properties of ELG are advantageous for simplifying the analysis of the folding reaction. Furthermore, the stable MG state of ELG observed at acid pH (A state) gives an opportunity to investigate the structure of the folding intermediate in detail if it is identical to the folding intermediate. To clarify whether an intermediate with

† This work was supported in part by a Grant-in-Aid for Scientific Research on Priority Areas from the Ministry of Education, Science, Sports and Culture of Japan.

* To whom correspondence should be addressed at the Department of Bioengineering, Faculty of Engineering, Soka University, 1-236 Tangi-cho, Hachioji, Tokyo 192-8577, Japan. Telephone 426-91-9444; Fax: 426-91-2317; E-mail: ikeguchi@t.soka.ac.jp.

‡ Soka University.

§ University of Tokyo.

[1] Abbreviations: BLG, bovine β-lactoglobulin; ELG, equine β-lactoglobulin; MG, molten globule; CD, circular dichroism; SAXS, small-angle X-ray scattering; GdnHCl, guanidine hydrochloride.

10.1021/bi982683p CCC: $18.00
Published on Web 03/19/1999

nonnative α-helices is kinetically formed in the folding reaction of ELG as observed for BLG and, if so, whether the kinetic intermediate is identical with the A state, we have investigated the folding and unfolding reactions of ELG using a stopped-flow method.

MATERIALS AND METHODS

Materials. ELG (component I) was prepared as previously described (*10*). Urea and guanidine hydrochloride (GdnHCl) were a specially prepared reagent grade from Nacalai Tesque. Other chemicals were analytical grade from Nacalai Tesque or Wako Pure Chemical Industries.

Equilibrium Experiments. The urea-induced equilibrium unfolding transitions of ELG were measured by difference absorption, fluorescence, and CD spectroscopies at pH 4.0 (50 mM citrate buffer) and 25 °C. The GdnHCl-induced unfolding transition was also measured by CD at pH 4.0 (50 mM formate buffer) and 25 °C. The protein concentration was 30−35 μM for the CD and absorbance measurements and 4.3 μM for the fluorescence measurements, which was spectrophotometrically determined using the molar extinction coefficient at 280 nm, $\epsilon_{280} = 12\,000\ M^{-1}\ cm^{-1}$ (*10*). The CD spectrum was measured on a Jasco J-720 spectropolarimeter. The path length of the optical cuvette was 1 mm or 10 mm for measurements of the far- or near-UV regions, respectively. The absorption and fluorescence spectra were measured with a Shimadzu UV-2200 spectrophotometer and a Shimadzu RF-5000 spectrofluorometer, respectively. The concentrations of urea and GdnHCl were determined from the refractive index (*14*).

Kinetic Experiments. The refolding and unfolding reactions were initiated by diluting an unfolded protein solution containing 8.0 M urea and a native protein solution, respectively, into a buffer (pH 4.0) solution containing an appropriate concentration of urea at 25 °C.

Stopped-flow fluorescence measurements were performed as previously described (*15*). The mixing ratio of the protein and diluent solutions was 1:9. The final protein concentration was 4.5 μM. The excitation wavelength was 295 nm (spectral bandwidth 3.5 nm) and the emission light through a 370-nm cutoff filter was observed. The dead time of the measurements was 2 ms. Under some conditions, the unfolding reactions were initiated by manual mixing and monitored by a change in fluorescence intensity at 320 nm using a Shimadzu RF-5000 spectrofluorometer.

Stopped-flow CD measurements were carried out using a stopped-flow apparatus (specially constructed by Unisoku Inc., Osaka) attached to a Jasco J-720 spectropolarimeter (*16*). In this experiment, 50 mM formate buffer was used instead of the citrate buffer in order to improve the signal-to-noise ratio (S/N). Both the equilibrium and kinetic CD data were confirmed to be independent of the buffers. The mixing ratio of the protein and diluent solutions was 1:10. The path length of the optical cell was 4 mm. The dead time of the measurements was 25 ms. The final protein concentrations were about 8 μM unless otherwise described. A 1-mm cell was also used to measure the protein concentration dependence of the refolding kinetics. In this case, the dead time of the measurements was 15 ms.

RESULTS

Unfolding Equilibrium. Figure 1a shows the difference absorption spectra, which were obtained by subtracting the absorption spectrum in the absence of urea from the spectrum at a given concentration of urea. The negative peaks around 290 nm and the positive peaks around 260 nm arise from the shift of the absorption spectrum of ELG to a shorter wavelength with increasing urea concentration, indicating that aromatic side chains are exposed to the solvent. From the molar absorption change at 287 nm ($\Delta\epsilon_{287}$), we obtained the urea-induced unfolding transition curve (Figure 2a), which indicates that ELG cooperatively unfolds around 3.2 M. Beyond 4 M urea, there is no spectrum change.

Figure 1b shows the urea concentration dependence of the fluorescence emission spectrum of ELG. Because the excitation wavelength is 295 nm, the spectrum change is expected to reflect the environmental change of Trp19, which is the only tryptophan residue present in ELG. The fluorescence spectrum has a maximum at 330 nm in the absence of urea and shows a red shift upon increasing urea concentration, suggesting that Trp19 is exposed to a more hydrophilic environment. The spectra obtained at urea concentrations from 0 to 4 M show an isoemission point at 350 nm, indicating that the urea-induced unfolding is a two-state transition in this concentration range of urea. However, the fluorescence spectrum no longer shows an isoemission point beyond 4 M, and the fluorescence intensity at 355 nm increases with urea concentration. Figure 2b shows the urea concentration dependence of the fluorescence intensity at 320 nm.

The CD spectra of ELG at various urea concentrations were measured in the near- and far-UV regions at pH 4.0 and 25 °C. The near-UV CD spectrum of the native ELG has three minima at 276, 286, and 293 nm, indicating the anisotropic environment of the aromatic side chains in the native conformation (Figure 1c). Upon increasing urea concentration, these aromatic signals cooperatively disappear as shown in Figure 2c. The urea-induced unfolding transition monitored by the ellipticity at 293 nm ($[\theta]_{293}$) almost coincides with those monitored by the absorption at 287 nm and the fluorescence at 320 nm.

The far-UV CD spectrum of the native ELG is typical of a β-sheet protein (Figure 1d). Interestingly, the CD ellipticity in the far-UV region cooperatively decreases with increasing urea concentration up to 3.7 M and then gradually increases beyond 4 M urea. The urea concentration dependence of the ellipticity at 222 nm ($[\theta]_{222}$) is presented in Figure 2d. To address whether the decrease in the ellipticity at 3.7 M urea is due to aggregation, the CD spectrum was measured at a lower protein concentration. The spectra at the lower protein concentration coincide with those at higher protein concentrations (Figure 2d), indicating that the decrease in the ellipticity at 3.7 M urea is not due to aggregation but is an indication of the population of an intermediate that probably has excess α-helices. The CD spectrum at 3.7 M urea is similar to that of the A state previously observed at pH 1.5 (*10*).

We have also examined the GdnHCl-induced equilibrium unfolding by CD at 25 °C and pH 4.0. The result is similar to that of the urea-induced unfolding experiment and indicates the presence of an intermediate (Figure 3). The

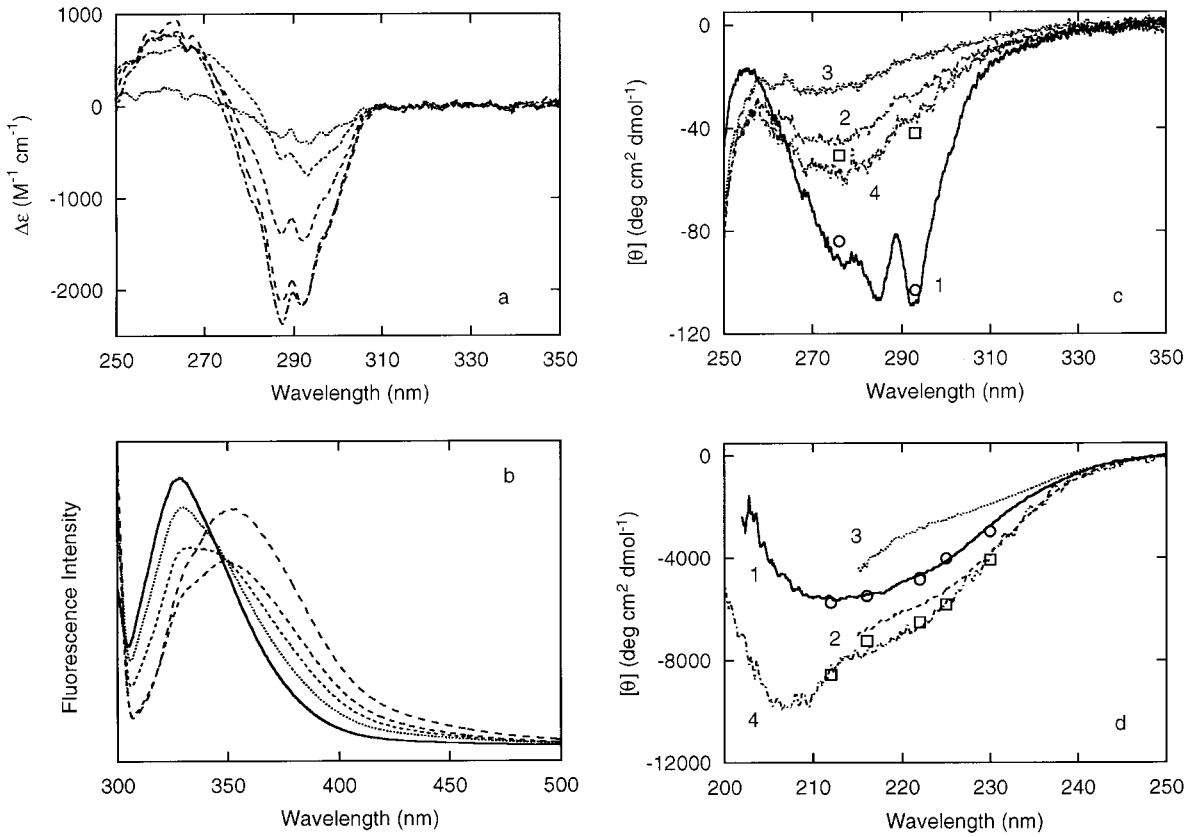

FIGURE 1: Urea-induced change in the difference absorption (a), fluorescence (b), near-UV CD (c), and far-UV CD (d) spectra of ELG at pH 4.0 and 25 °C. Shown in panel a are the spectra at 2.6, 3.0, 3.3, 4.0, and 8.1 M urea, reading downward at 290 nm. The fluorescence spectra at 0, 3.0, 3.4, 4.0, and 8.0 M (reading upward at 380 nm) are shown in panel b. In panels c and d, CD spectra at 0 M (curve 1), 3.7 M (curve 2), and 8.0 M (curve 3) are shown with the spectrum of the MG state in 0.1 M HCl−KCl, pH 1.5 (curve 4). In panels c and d, the initial (□) and final (○) ellipticities of the refolding reaction at 0.7 M urea are also shown (see text).

posttransition baseline is more clearly observed in the GdnHCl-induced unfolding monitored by $[\theta]_{222}$ than in the urea-induced unfolding.

Analysis of Unfolding Equilibrium. As shown above, the denaturant-induced unfolding transition monitored by the far-UV CD spectrum indicates the existence of at least one intermediate that has a far-UV CD value more negative than that of the native state. Thus, we assume, as the simplest model, the three-state transition between the native (N), intermediate (I), and unfolded (U) states:

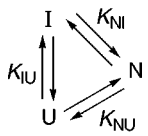

(1)

where K_{ij} is the equilibrium constant between the i and j states. The free energy difference between the i and j states, ΔG_{ij}, is assumed to be a linear function of the denaturant concentration, $[c]$:

$$\Delta G_{ij} = -RT \ln K_{ij} = -RT \ln(f_j/f_i) = \Delta G_{ij}^{H_2O} - m_{ij}[c] \quad (2)$$

where R is the gas constant, T is the absolute temperature, f_i and f_j are the populated fractions of the i and j states, respectively, $\Delta G_{ij}^{H_2O}$ is the free energy change of the $i \rightleftarrows j$ transition in the absence of denaturant, and m_{ij} reflects the cooperativity of the transition. On the basis of these assumptions, the unfolding transition curve is represented by

$$\theta_{obs} = f_N\theta_N + f_I\theta_I + f_U\theta_U$$
$$= [\theta_N \exp\{(\Delta G_{NU}^{H_2O} - m_{NU}[c])/RT\} + \theta_I \exp\{(\Delta G_{IU}^{H_2O} - m_{IU}[c])/RT\} + \theta_U]/[1 + \exp\{(\Delta G_{NU}^{H_2O} - m_{NU}[c])/RT\} + \exp\{(\Delta G_{IU}^{H_2O} - m_{IU}[c])/RT\}] \quad (3)$$

where θ_N, θ_I, and θ_U are the spectral properties of the N, I, and U states, respectively. The thermodynamic parameters in eq 3, $\Delta G_{NU}^{H_2O}$, $\Delta G_{IU}^{H_2O}$, m_{NU}, and m_{IU}, that allow simultaneous fitting of a function represented by eq 3 to both transition curves monitored by $[\theta]_{293}$ and $[\theta]_{222}$ were obtained by a global fitting program. In this calculation, θ_N, θ_I, and θ_U at 293 nm were assumed to be independent of denaturant concentration. The θ_N and θ_I at 222 nm were also assumed to be independent of the denaturant concentration (this assumption has been revealed to be valid by kinetic experiments shown below). Because the $[\theta]_{222}$ value of the U state, θ_U, apparently depends on the denaturant concentration, we have assumed that it linearly depends on the denaturant concentration $[c]$:

$$\theta_U = \theta_U^{H_2O} + \Delta\theta_U[c] \quad (4)$$

where $\theta_U^{H_2O}$ is the θ_U value in the absence of the denaturant and $\Delta\theta_U$ is the dependence of θ_U on $[c]$. The optimized

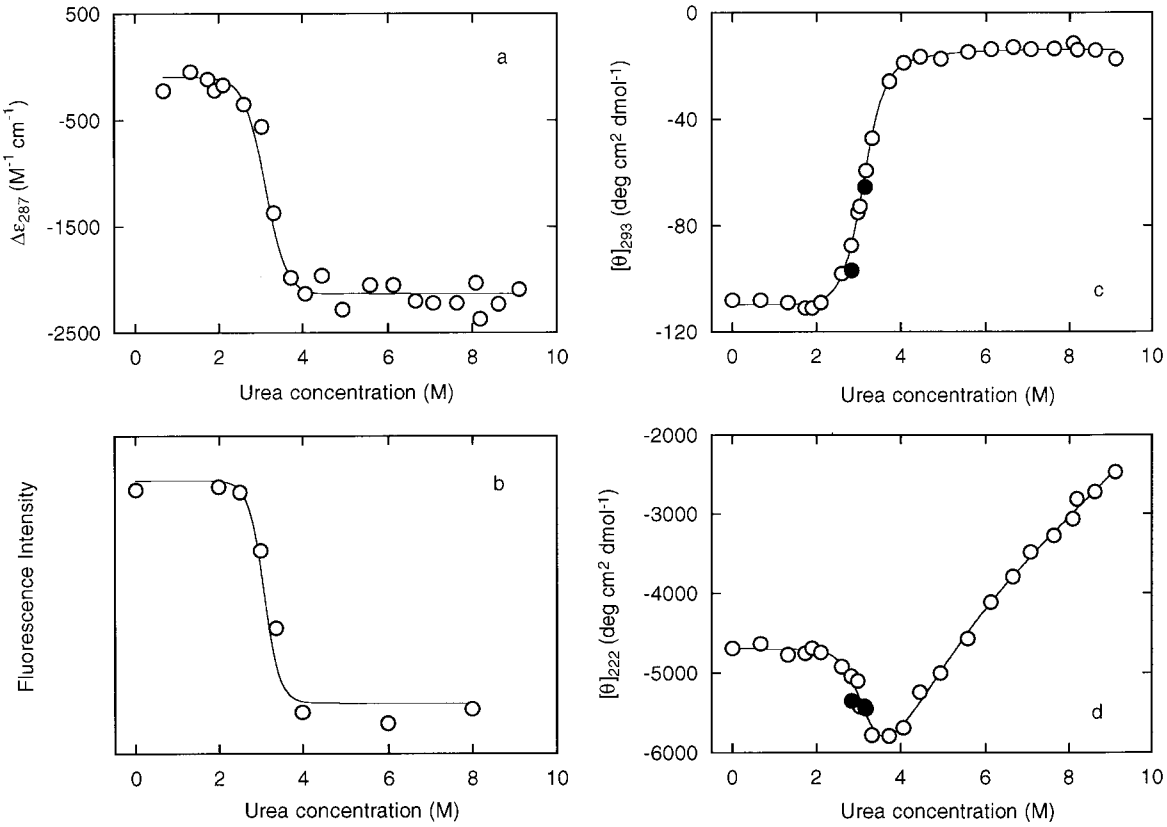

FIGURE 2: Urea-induced unfolding transitions monitored by (a) molar absorption difference at 287 nm, (b) fluorescence intensity at 320 nm, (c) $[\theta]_{293}$, and (d) $[\theta]_{222}$. In panels c and d, open and closed circles denote the data at protein concentrations of 30−35 μM and 8.4 μM, respectively. The solid lines in panels c and d are the best-fit curves based on eq 3, of which the fitted parameters are $\theta_N = -110 \pm 1$ deg·cm^2/dmol, $\theta_I = -22 \pm 3$ deg·cm^2/dmol, $\theta_U = -14 \pm 1$ deg·cm^2/dmol at 293 nm, $\theta_N = -4695 \pm 47$ deg·cm^2/dmol, $\theta_I = -6407 \pm 335$ deg·cm^2/dmol, $\theta_U^{H_2O} = -7096 \pm 66$ deg·cm^2/dmol, $\Delta\theta_U = 511 \pm 41$ deg·cm^2/(dmol·M) at 222 nm, $\Delta G_{NU}^{H_2O} = 9.83 \pm 1.27$ kcal/mol, $m_{NU} = 2.90 \pm 0.31$ kcal/(mol·M), $\Delta G_{IU}^{H_2O} = 2.90 \pm 1.09$ kcal/mol, and $m_{IU} = 0.74 \pm 0.21$ kcal/(mol·M). Solid lines in panels a and b are the fitting curves from a modified version of eq 3 in which $\theta_I = \theta_U$ and the parameters $\Delta G_{NU}^{H_2O}$, m_{NU}, $\Delta G_{IU}^{H_2O}$, and m_{IU} are fixed at the above values.

parameters are shown in Table 1 and the legends of Figures 2 and 3, and the fitting curves calculated with these parameters are shown as solid lines in Figures 2c,d and 3. Although the transitions monitored by the absorbance and fluorescence spectra were not included in the fitting because these transitions coincide with the transition measured by $[\theta]_{293}$, we have constructed the theoretical transition curves monitored by these aromatic probes using a modified version of eq 3 in which θ_I is assumed to be identical with θ_U and the thermodynamic parameters are fixed to the values obtained above. The theoretical curves coincide with the observed ones (Figure 2a,b), indicating that the three-state model can reasonably describe all equilibrium data. Furthermore, the values of $\Delta G_{NU}^{H_2O}$ and $\Delta G_{IU}^{H_2O}$ estimated from the urea-induced unfolding curve are the same within experimental errors as the values from the GdnHCl-induced unfolding curve (Table 1), suggesting the validity of the three-state model.

Refolding and Unfolding Kinetics. Figure 4 shows the changes in the fluorescence and the ellipticities at 293 and 222 nm during the refolding of ELG initiated by a urea-concentration jump from 8 to 0.7 M at 25 °C and pH 4.0. The refolding reaction was also monitored by CD at 276 nm and several wavelengths between 212 and 230 nm. All the refolding curves have been analyzed by a nonlinear least-squares curve fitting. The kinetic curve obtained by the fluorescence change is represented by at least three exponential terms with rate constants of 4.6 s^{-1} (fast phase), 0.78 s^{-1} (middle phase), and 0.13 s^{-1} (slow phase). The kinetic curves obtained by the far-UV CD are also represented by at least three exponential terms with rate constants similar to those obtained by fluorescence (Table 2). To examine whether aggregation occurs during the refolding kinetics, the refolding kinetics has been measured by $[\theta]_{222}$ at protein concentrations ranging from 8 to 27 μM in a stopped-flow cell of 1 mm path length. No dependence on the protein concentration was observed, suggesting the absence of protein aggregation (data not shown). Thus, the refolding experiments to measure the near-UV ellipticity change have been performed at a protein concentration of 27 μM, because the CD intensity in the near-UV region is much weaker than that in the far-UV region. The refolding kinetics detected by the near-UV CD is well represented by two exponential terms with rate constants similar to those of the middle and slow phases observed by fluorescence and far-UV CD (Table 2).

Furthermore, it is notable that a significant CD change occurs within the dead time of the measurement (burst phase). When the refolding reaction is started from the unfolded state in 8 M urea to the native state, it is expected that the CD ellipticity at 222 nm decreases from the value of the unfolded state in 8 M urea ($[\theta]_{222} = -3010$ deg cm^2 dmol^{-1}) to that of the native state ($[\theta]_{222} = -4700$ deg cm^2 dmol^{-1}). Upon refolding, however, the CD value more

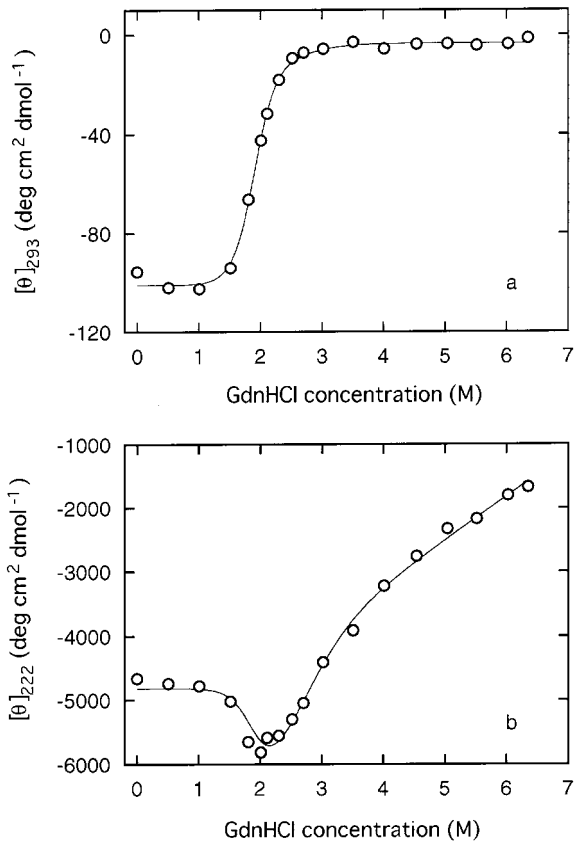

FIGURE 3: GdnHCl-induced unfolding transitions monitored by (a) $[\theta]_{293}$ and (b) $[\theta]_{222}$ at pH 4.0 and 25 °C. The solid lines are the best-fit curves based on eq 3, of which the fitted parameters are $\theta_N = -101 \pm 1$ deg·cm^2/dmol, $\theta_I = -14 \pm 4$ deg·cm^2/dmol, $\theta_U = -3 \pm 1$ deg·cm^2/dmol at 293 nm, $\theta_N = -4811 \pm 69$ deg·cm^2/dmol, $\theta_I = -6407$ deg·cm^2/dmol (assumed to be the same as the value in the urea-induced unfolding), $\theta_U{}^{H_2O} = -5927 \pm 130$ deg·cm^2/dmol, $\Delta\theta_U = 686 \pm 129$ deg·cm^2/(dmol·M) at 222 nm, $\Delta G_{NU}{}^{H_2O} = 10.06 \pm 0.93$ kcal/mol, $m_{NU} = 4.74 \pm 0.44$ kcal/mol/M, $\Delta G_{IU}{}^{H_2O} = 3.92 \pm 0.74$ kcal/mol, and $m_{IU} = 1.54 \pm 0.28$ kcal/(mol·M).

negative than that of the native state is attained within the dead time of the measurement and then the CD value increases to that of the native state by a relaxation represented by three exponential terms. This result suggests that an intermediate with a higher far-UV CD intensity is formed in the burst phase. In the near-UV region, a change within the dead time also occurs, although the CD intensity does not exceed the value of the native state.

The urea concentration dependence of the folding and unfolding rate has been investigated by CD at 222 nm. Figure 5 shows the urea concentration dependence of the apparent folding and unfolding rate constants. The rates of the three refolding phases decrease with increasing urea concentration. The amplitudes of the fast and middle phases observed at 0.7 M urea decrease with increasing urea concentration and disappear around 3 M urea. The unfolding reaction is well represented as a single-exponential kinetics at all urea concentrations, and its rate increases with urea concentration. The refolding rate coincides with the unfolding rate at the midpoint of the equilibrium transition (3.2 M urea). This V-shape dependence of the apparent folding−unfolding rate on the denaturant concentration is generally observed for many proteins that fold by the two-state mechanism (for a recent review, see ref *17*). The clear "rollover" in the denaturant dependence of the folding rate, which is an indication of the presence of intermediates, is not observed. However, the urea concentration dependence of the apparent folding−unfolding rate (Figure 5) is not necessarily inconsistent with the presence of a folding intermediate, because the folding mechanism of ELG is quite complex, as discussed later.

Structure and Stability of the Burst Phase Intermediate. As described above, a significant ellipticity change occurs within the dead time of stopped-flow measurements during the folding reaction of ELG, suggesting the formation of a burst-phase intermediate. Because the relaxation that corresponds to the formation of the burst-phase intermediate is complete within the dead time of measurements (25 ms) and has not been observable, the rate constant of the formation of the burst-phase intermediate must be greater than 200 s^{-1}. Because the rate constant of the fastest observed relaxation is 4−9 s^{-1} (Table 2), the formation of the burst-phase intermediate is kinetically uncoupled from the subsequent folding phase. As described below, furthermore, the equilibrium between the burst-phase intermediate and the unfolded state is attained within the dead time. The initial ellipticity, which is obtained by extrapolating the observed folding curve to zero time, therefore gives the ellipticity of the burst-phase intermediate or the preequilibrium value of the transition between the intermediate and unfolded states. In Figure 1c,d, the initial ellipticities at 0.7 M urea obtained from the kinetic folding curves measured at various wavelengths are shown. To address whether the initial ellipticity at 0.7 M urea reflects the ellipticity of the burst-phase intermediate or the ellipticity of the equilibrium mixture of the burst-phase intermediate and the unfolded state, and to determine the stability of the burst-phase intermediate, the urea concentration dependence of the initial ellipticity at 222 nm was investigated (Figure 6). The initial ellipticity during refolding is constant from 0.7 to 3 M urea, indicating that the burst-phase intermediate is stable in this urea concentration range. Therefore, the wavelength dependence of the initial ellipticity at 0.7 M urea shown in Figure 1c,d is the CD spectrum of the burst-phase intermediate. The CD spectrum of the burst-phase intermediate is in good agreement with that of the A state in both the far- and near-UV regions, indicating that the burst-phase intermediate assumes a conformation indistinguishable from that in the A state.

Because the CD spectrum at 3.7 M urea is similar to that of the A state (Figure 1c,d), the I state observed during the urea-induced unfolding transition is also thought to be equivalent with the burst-phase intermediate. When the urea concentration jumps from 8 M to 4, 5, or 6 M, where both the I and U states populate, there is no ellipticity change in the observable time range, and the ellipticity attained within the dead time coincides with that of the equilibrium unfolding transition. This indicates that the I state observed during the equilibrium unfolding is equivalent with the burst-phase intermediate. Using the parameters obtained from the analysis of the equilibrium unfolding transition (Figure 2 caption), we can construct the I $\rightleftarrows$ U transition curve, which is shown in Figure 6. The curve shows a good agreement with the initial ellipticity during refolding below 3 M urea, indicating that the burst-phase intermediate shows the same urea-induced unfolding transition with the I state.

Table 1: Thermodynamic Parameters of ELG Unfolding at pH 4.0 and 25 °C

denaturant	$\Delta G_{NU}^{H_2O}$ (kcal/mol)	m_{NU} [kcal/(mol·M)]	$c_{NU}^{1/2}$ (M)[a]	$\Delta G_{IU}^{H_2O}$ (kcal/mol)	m_{IU} [kcal/(mol·M)]	$c_{IU}^{1/2}$ (M)[a]
urea	9.83 ± 1.27	2.90 ± 0.31	3.39 ± 0.57	2.90 ± 1.09	0.74 ± 0.21	3.94 ± 1.84
GdnHCl	10.06 ± 0.93	4.74 ± 0.44	2.12 ± 0.28	3.92 ± 0.74	1.54 ± 0.28	2.55 ± 0.67

[a] Denaturant concentration of the transition midpoint.

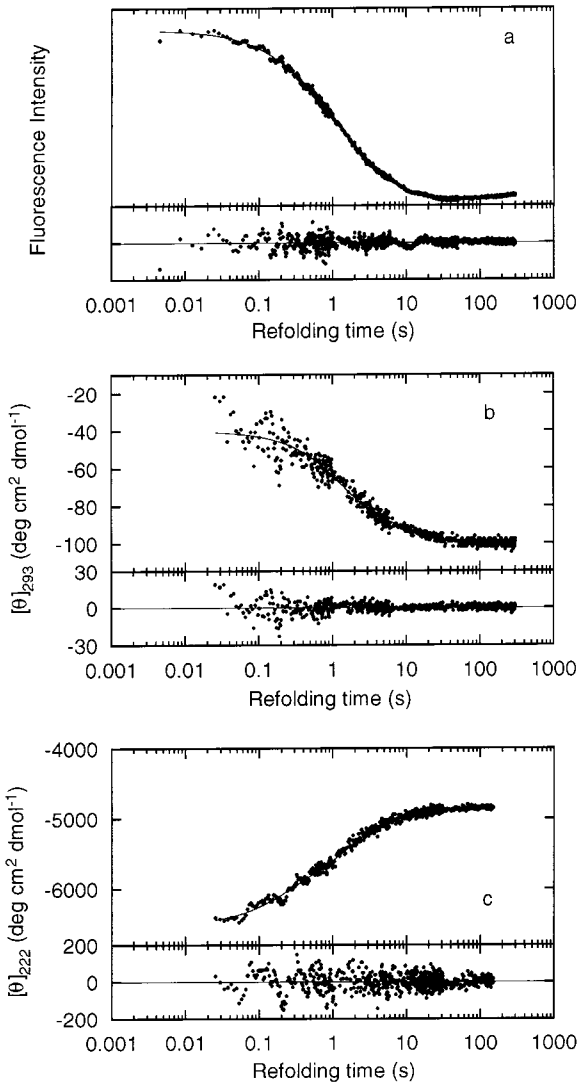

FIGURE 4: Refolding kinetics monitored by fluorescence at 0.8 M urea (a) and by $[\theta]_{293}$ (b) and $[\theta]_{222}$ (c) at 0.7 M urea, pH 4.0, and 25 °C. Residuals to the three- (a and c) and two- (b) exponential fitting curves are shown in the lower panels.

On the other hand, the initial ellipticity during the unfolding reaction is almost independent of the urea concentration, and the value is coincident with the ellipticity in the pretransition region of the equilibrium unfolding curve. This result indicates the absence of the unfolding intermediate between the native and transition states, and the assumption that the $[\theta]_{222}$ values of the N and I states (θ_N and θ_I) are independent of urea concentration is revealed to be valid.

Refolding from the Equilibrium Intermediate. To further confirm that the A and I states are equivalent with the burst-phase intermediate, the refolding kinetics from the A state or the equilibrium mixture of the I and U states at 4.5 M urea has been measured and compared with that from 8 M urea. Irrespective of the initial conditions, three kinetic phases are observed (Table 3). Both the rate constant and relative amplitude of each phase of the refolding kinetics from different initial conditions are the same within experimental error, indicating that the equilibrium between the intermediate and unfolded states is rapidly attained within the dead time of the measurements.

DISCUSSION

The Molten Globule State Is Equivalent with the Transient Folding Intermediate. In this study, an equilibrium intermediate (the I state) of ELG similar to the A state that has previously been observed at acid pH (*10*) was found at moderate denaturant concentrations. A gel-filtration experiment has shown that the I state is nearly as compact as the native conformation (unpublished results). A kinetic intermediate (burst-phase intermediate) was also detected during an early stage in the folding reaction of ELG. The following lines of experimental evidence indicate that both the A and I states are indistinguishable from the burst-phase folding intermediate: (1) The CD spectrum of the burst-phase intermediate is indistinguishable from that of the A state. (2) The CD spectrum of the I state is similar to those of the A state and the burst-phase intermediate. (3) The urea-induced unfolding transition of the burst-phase intermediate coincides with that of the I state. (4) The A and I states are kinetically indistinguishable from the burst-phase intermediate, because the refolding kinetics from the A and I states are the same as that from the U state.

Previously, we have detected a compact intermediate with nonnative α-helices during an early stage of the folding reaction of BLG (*4*, *5*, *7*). Although the existence of an equilibrium intermediate has been suggested in the denaturant-induced equilibrium unfolding of BLG, its population is low and its structural characterization has been limited (*5*, *7*, *18*−*20*). Therefore, ELG is a more useful protein for investigating the detailed structure of the burst-phase intermediate than BLG. The A state of ELG has been characterized to be a compact MG state in which both α-helix (20%) and β-sheet (28%) structures are formed and the tertiary packing of the side chains is lost (*10*). Further characterization of the structure in the A state by 2D NMR and hydrogen exchange is now in progress.

It is not surprising that the MG intermediate of BLG does not well populate at equilibrium. As demonstrated previously for α-lactalbumin and lysozyme (*8*) and for mutants of barnase (*21*), whether the intermediate can be detected at equilibrium is dependent on the relative stability among the native, intermediate, and unfolded states. The apparent difference in the equilibrium unfolding between BLG and ELG is probably due to the difference in the relative stability of the native state to the intermediate, although no exact comparison of the stability can be made because of the lack of the stability data under the same condition. The stability of BLG estimated under the conditions closest to those of the present study is that estimated from the urea-induced unfolding monitored by $[\theta]_{293}$ at pH 3.2 and 25 °C (*7*).

Table 2: Rate Constants and Relative Amplitudes of Folding of ELG at 0.7 M Urea, pH 4.0 and 25 °C

	rate constants (s^{-1})			relative amplitudes (%)			
							slow
probe	slow	middle	fast	slow	middle	fast	slow + middle
fluorescence[a]	0.135 ± 0.004	0.78 ± 0.02	4.6 ± 0.3	26 ± 1	57 ± 1	17 ± 1	31 ± 1
CD at 293 nm	0.076 ± 0.008	0.77 ± 0.05		30 ± 2	70 ± 2		30 ± 1
CD at 276 nm	0.086 ± 0.007	0.74 ± 0.06		44 ± 2	56 ± 2		44 ± 1
CD at 230 nm	0.068 ± 0.010	0.53 ± 0.04	4.1 ± 0.5	14 ± 2	54 ± 2	32 ± 2	21 ± 2
CD at 225 nm	0.081 ± 0.009	0.67 ± 0.04	7.0 ± 0.9	16 ± 1	56 ± 1	28 ± 1	22 ± 1
CD at 222 nm	0.090 ± 0.009	0.67 ± 0.04	6.0 ± 0.7	18 ± 1	55 ± 1	27 ± 1	24 ± 1
CD at 216 nm	0.088 ± 0.018	0.70 ± 0.07	8.9 ± 2.1	17 ± 2	58 ± 3	25 ± 2	22 ± 3
CD at 212 nm	0.075 ± 0.014	0.67 ± 0.08	9.0 ± 1.7	17 ± 2	48 ± 2	35 ± 3	26 ± 3

[a] Urea concentration is 0.8 M.

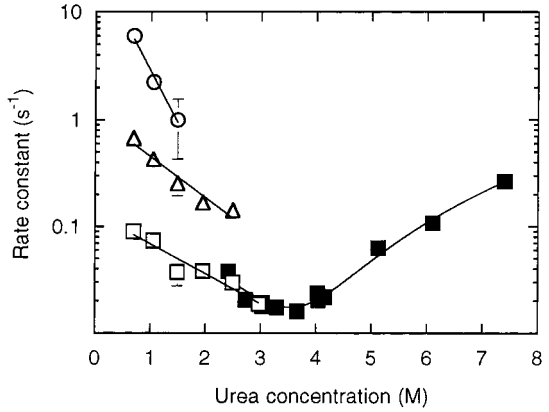

FIGURE 5: Urea concentration dependence of the folding and unfolding rate. The rate constants of the fast (○), middle (△), and slow (□) phases in refolding reactions and the rate constants of the unfolding reactions (■) are shown.

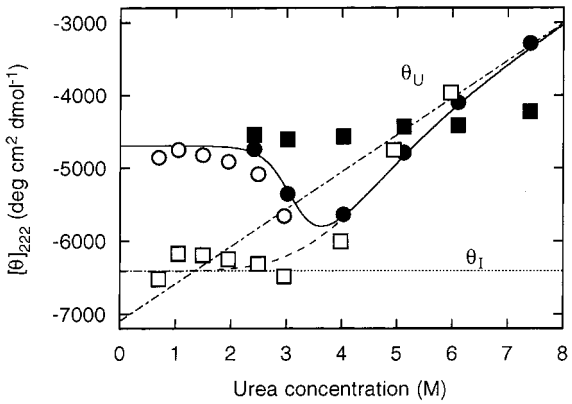

FIGURE 6: Initial (□, ■) and final (○, ●) ellipticities of unfolding (closed symbols) and refolding (open symbols) kinetics at various urea concentrations. Solid line is the equilibrium unfolding transition curve, which is a reproduction of the fitting curve shown in Figure 2d. Dashed line is a theoretical I ⇄ U transition curve drawn with the parameters shown in Figure 2.

Because the population of the intermediate is quite low and the three-state analysis of the unfolding equilibria is not possible for BLG, we compare here the free energy change of unfolding monitored by $[\theta]_{293}$ and analyzed by the two-state model (ΔG_{app}). Because the ellipticity change at 293 nm reflects mainly the N ⇄ I transition, ΔG_{app} should be close to ΔG_{NI}. When the present data shown in Figure 2c were analyzed by the two-state model, we obtained the values of 6.73 kcal/mol for ΔG_{app} and 2.14 kcal/(mol·M) for the cooperativity parameter m_{app}. These values are similar to ΔG_{NI} (= $\Delta G_{NU} - \Delta G_{IU}$ = 6.93 kcal/mol) and m_{NI} [= $m_{NU} - m_{IU}$ = 2.16 kcal/(mol·M)], respectively. On the other hand, ΔG_{app} and m_{app} of BLG were reported to be 10.4 and 2.22 kcal/(mol·M) (*7*). The similarity of the m_{app} value between BLG and ELG is consistent with the homologous structure of these proteins. However, ΔG_{app} of BLG is much larger than that of ELG, indicating that the native structure of BLG is more stable than that of ELG.

Kinetic Role of the Burst-Phase Intermediate. To clarify whether the formation of nonnative α-helices is crucial for directing the subsequent folding process, the kinetic role of the burst-phase intermediate must be established. As stated by Creighton (*22*), it is difficult to establish definitively the kinetic role of the burst-phase intermediate. If the intermediate is an on-pathway and obligatory one, there should be a lag period in the appearance of the N state. However, the lag period has not been detected, because the formation of the burst-phase intermediate is too fast to be observed by the stopped-flow apparatus used in this study. An alternative way to address the kinetic role of the burst-phase intermediate is to examine whether the rate of the appearance of the N state correlates with the population of the intermediate. Recently, we have examined the GdnHCl concentration dependence of the folding rate and the population of the MG intermediate of bovine α-lactalbumin and have concluded that the MG intermediate of this protein is not an obligatory folding intermediate (*23*). On the other hand, it has been shown for ribonuclease H and equine lysozyme that the denaturant concentration dependence of the folding rate is well described with a model in which the MG intermediate is an obligatory intermediate (*24*−*26*). In the case of ELG, however, there are three kinetic phases after the burst phase, in contrast to the cases of above proteins where only a single-exponential process is observed after the burst phase. To address whether there is a correlation between the folding rate and the population of the MG intermediate, it must be clarified whether each of three kinetic phases observed after the burst phase reflects the sequential folding reaction with a series of intermediates or parallel pathways, all of which produce the N state.

Folding Kinetics of β-Lactoglobulin. The folding kinetics of ELG is complex and there are at least four kinetic phases: the burst, fast, middle, and slow phases. In the burst phase, the MG intermediate is formed. In the MG intermediate, 20% and 28% of residues have been estimated to assume α-helix and β-sheet structures, respectively (*10*). Because the native structure has 9% α-helix and 41% β-sheet (*10*), at least 11% of the residues assumes nonnative α-helices in the MG state. It is clear, therefore, that the nonnative

Table 3: Comparison of Refolding Kinetics from Different Initial Conditions[a]

initial conditions	rate constants (s^{-1})			relative amplitudes (%)		
	slow	middle	fast	slow	middle	fast
50 mM formate, 8 M urea (pH 4)	0.090 ± 0.009	0.67 ± 0.04	6.0 ± 0.7	18 ± 1	55 ± 1	27 ± 1
50 mM formate, 4.5 M urea (pH 4)	0.091 ± 0.016	0.55 ± 0.07	5.3 ± 0.7	18 ± 3	45 ± 2	38 ± 2
0.1 M HCl−KCl (pH 1.5)	0.096 ± 0.012	0.59 ± 0.08	4.3 ± 0.5	22 ± 2	41 ± 2	37 ± 2

[a] The final conditions after the mixing were 50 mM formate (pH 4.0) and 0.7 M urea at 25 °C.

α-helices unfold or are converted to the native β-sheet structure during the late three kinetic phases (fast, middle, and slow). Even though the regions that assume nonnative α-helices in the MG state are converted to the β-sheet structure in the N state, the nonnative α-helices must transiently unfold. Which phase of the subsequent three kinetic phases corresponds to the unfolding of the nonnative α-helices? Do the subsequent three kinetic phases represent the sequential folding reaction with a series of intermediates with different secondary structural contents or parallel pathways that are originated because of circumstances such as the cis−trans isomerization of X−Pro peptide bonds in the MG state? The fast phase is observed by fluorescence and far-UV CD but is not detected by near-UV CD. This result indicates that the fast-phase reflects the formation of an intermediate of which the near-UV CD spectrum is the same as that of the MG intermediate but the fluorescence and far-UV CD spectra are different from those of both the MG and N states. From these spectral properties, this fast phase intermediate is supposed to have a slightly reduced α-helical content than MG and an environment of Trp19 different from that of MG. If the nonnative α-helices of the MG state are completely unfolded in the fast-phase intermediate, the far-UV CD should decrease or not change in the middle and slow phases because at least 13% of the residues must acquire the native β-sheet structure during the three observable kinetic phases. The result in which the far-UV CD increases during the middle and slow phases therefore indicates that a part of the nonnative α-helices remains in the fast-phase intermediate. It is difficult, however, to estimate quantitatively the secondary structural contents in the fast-phase intermediate, because our kinetic CD data are limited to wavelengths longer than 212 nm due to the insufficient S/N. The middle and slow phases are observed by all spectral probes. The relative amplitudes of these phases are independent of wavelength in the far-UV CD (Table 2), suggesting that the middle and slow phases correspond to the parallel pathways. The amplitude ratios between the slow and middle phases detected by fluorescence and near-UV CD, however, are slightly higher than those monitored by the far-UV CD. These results may suggest the existence of the middle-phase intermediate, although the possibility that the middle and slow phases represent the parallel folding pathway cannot be ruled out.

It is notable that the complete refolding of BLG takes a much longer time than that of ELG (*5*, *7*). At least six kinetic phases have been observed for the refolding of BLG at 0.4 M GdnHCl, pH 3.2 and 4.5 °C (*5*) and at 3 M urea, pH 3.2 and 25 °C (*7*), in contrast to four kinetic phases observed for ELG in this study. The slowest phase of BLG refolding has a rate constant 2 or 3 orders of magnitude lower than that in ELG refolding and is detected only by aromatic absorption and CD. Such a slow phase is absent during the refolding of ELG. BLG and ELG have several different properties. ELG is monomeric at pH 3−8 (*10*), whereas BLG forms a dimer at neutral pH (*12*). Both proteins have two disulfide bonds (Cys66−Cys160 and Cys106−Cys119), and BLG has a free cysteine at position 121 that is absent in ELG. Our previous studies of BLG have been performed under an acidic condition where BLG is monomeric and a thiol−disulfide interchange reaction is expected to be suppressed. In fact, SAXS experiments have shown the absence of the dimer throughout the refolding reaction of BLG and exclude the possibility that the slowest folding phase of BLG resulted from the dimer formation (*7*). However, the possibility has not been ruled out that the slowest folding phase of BLG is related to a thiol−disulfide interchange reaction. Further studies on both BLG and ELG will clarify the folding mechanism of β-lactoglobulin.

ACKNOWLEDGMENT

We thank Professor Shinji Takai of the Department of Veterinary, Kitasato University, who kindly supplied the equine milk.

REFERENCES

1. Flower, D. R., North, A. T. C., and Attwood, T. K. (1993) *Protein Sci. 2*, 753−761.
2. Banaszak, L., Winter, N., Xu, Z., Bernlohr, D. A., Cowan, S., and Jones, T. A. (1994) *Adv. Protein Chem. 45*, 89−151.
3. Flower, D. R. (1996) *Biochem. J. 318*, 1−14.
4. Kuwajima, K., Yamaya, H., Miwa, S., Sugai, S., and Nagamura, T. (1987) *FEBS Lett. 221*, 115−118.
5. Kuwajima, K., Yamaya, H., and Sugai, S. (1996) *J. Mol. Biol. 294*, 806−822.
6. Hamada, D., Segawa, S., and Goto, Y. (1996) *Nat. Struct. Biol. 3*, 868−873.
7. Arai, M., Ikura, T., Semisotnov, G. V., Kihara, H., Amemiya, Y., and Kuwajima, K. (1998) *J. Mol. Biol. 275*, 149−162.
8. Kuwajima, K. (1989) *Proteins*: *Struct., Funct., Genet. 6*, 87−103.
9. Ptitsyn, O. B. (1995) *Adv. Protein Chem. 47*, 83−229.
10. Ikeguchi, M., Kato, S., Shimizu, A., and Sugai, S. (1997) *Proteins: Struct., Funct., Genet. 27*, 567−575.
11. Conti, A., Godovac-Zimmermann, J., Liberatori, J., and Braunitzer, G. (1984) *Hoppe-Seyler's Z. Physiol. Chem. 365*, 1393−1401.
12. McKenzie, H. A. (1967) *Adv. Protein Chem. 22*, 55−234.
13. McKenzie, H. A., Ralston, G. B., and Shaw, D. C. (1972) *Biochemistry 11*, 4539−4547.
14. Pace, C. N. (1986) *Methods Enzymol. 131*, 266−280.
15. Arai, M., and Kuwajima, K. (1996) *Folding Des. 1*, 275−287.
16. Kuwajima, K. (1996) in *Circular Dichroism and the Conformational Analysis of Biomolecules* (Fasman, G. D., Ed.) pp 159−182, Plenum, New York.
17. Clarke, A. R., and Waltho, J. P. (1997) *Curr. Opin. Biotechnol. 8*, 400−410.
18. Pace, C. N., and Tanford, C. (1968) *Biochemistry 7*, 198−208.

19. Ananthanarayanan, V. S., and Ahmad, F. (1977) *Can. J. Biochem. 55*, 239−243.
20. Hamada, D., and Goto, Y. (1997) *J. Mol. Biol. 269*, 479−487.
21. Sanz, J. M., and Fersht, A. R. (1993) *Biochemistry 32*, 13584−13592.
22. Creighton, T. E. (1997) *Trends Biochem. Sci. 22*, 6−11.
23. Ikeguchi, M., Fujino, M., Kato, M., Kuwajima, K., and Sugai, S. (1998) *Protein Sci. 7*, 1564−1574.
24. Yamasaki, K., Ogasahara, K., Yutani, K., Oobatake, M., and Kanaya, S. (1995) *Biochemistry 34*: 16552−16562.
25. Raschke, T. M., and Marqusee, S. (1997) *Nat. Struct. Biol. 4*, 298−304.
26. Mizuguchi, M., Arai, M., Ke, Y., Nitta, K., and Kuwajima, K. (1998) *J. Mol. Biol. 283*, 265−277.

BI982683P